Long-term FXa inhibition attenuates thromboinflammation after acute myocardial infarction and stroke by platelet proteome alteration

Amin Polzin, Marcel Benkhoff, Manuela Thienel, Maike Barcik, Philipp Mourikis, Khrystyna Shchurovska, Carolin Helten, Vincent Ehreiser, Zhang Zhe, Franziska von Wulffen, Alexander Theiss, Sameera Peri, Sophie Cremer, Samantha Ahlbrecht, Saif Zako, Laura Wildeis, Gabrielle Al-Kassis, Daniel Metzen, Amelie Utz, Hao Hu, Lilian Vornholz, Goran Pavic, Enzo Lüsebrink, Jan Strecker, Steffen Tiedt, Mareike Cramer, Michael Gliem, Tobias Ruck, Sven G. Meuth, Tobias Zeus, Christoph Mayr, Herbert B. Schiller, Lukas Simon, Steffen Massberg, Malte Kelm, Tobias Petzold

Article - Version of Record

Received: 19 April 2024 | Revised: 8 October 2024 | Accepted: 16 October 2024

https://doi.org/10.1016/j.jtha.2024.10.025

ORIGINAL ARTICLE

Long-term FXa inhibition attenuates thromboinflammation after acute myocardial infarction and stroke by platelet proteome alteration

Amin Polzin[1,2,3] | Marcel Benkhoff[1,4] | Manuela Thienel[5,6] | Maike Barcik[1] | Philipp Mourikis[1] | Khrystyna Shchurovska[5,6] | Carolin Helten[1] | Vincent Ehreiser[7,8,9] | Zhang Zhe[5,6] | Franziska von Wulffen[5,6] | Alexander Theiss[5,6] | Sameera Peri[5,6] | Sophie Cremer[1] | Samantha Ahlbrecht[1] | Saif Zako[1] | Laura Wildeis[1] | Gabrielle Al-Kassis[1] | Daniel Metzen[1] | Amelie Utz[1] | Hao Hu[1] | Lilian Vornholz[1] | Goran Pavic[10] | Enzo Lüsebrink[5,6] | Jan Strecker[5] | Steffen Tiedt[11] | Mareike Cramer[1] | Michael Gliem[10] | Tobias Ruck[10] | Sven G. Meuth[10] | Tobias Zeus[1] | Christoph Mayr[12,13] | Herbert B. Schiller[12,13] | Lukas Simon[14,15] | Steffen Massberg[5,6] | Malte Kelm[1,2] | Tobias Petzold[7,8,9]

[1]Department of Cardiology, Pulmonology, and Vascular Medicine, University Hospital Düsseldorf, Medical Faculty of the Heinrich Heine University Düsseldorf, Düsseldorf, Germany

[2]Cardiovascular Research Institute Düsseldorf (CARID), Medical Faculty and University Hospital, Düsseldorf, Germany

[3]National Heart and Lung Institute, Imperial College London, London, United Kingdom

[4]Institute of Analytical Chemistry, University of Vienna, Vienna, Austria

[5]Department of Cardiology, Ludwig-Maximilians-University Hospital, Ludwig Maximilians University, Munich, Germany

[6]Deutsches Herzzentrum der Charité (German Centre for Cardiovascular Research), Munich Heart Alliance, Munich, Germany

[7]Deutsches Herzzentrum der Charité University Hospital Berlin, Department of Cardiology, Angiology and Intensive Care Medicine, Campus Benjamin Franklin, Hindenburgdamm 30, 12203 Berlin, Germany

[8]Deutsches Herzzentrum der Charité (German Centre for Cardiovascular Research), Partner site Berlin, Berlin, Germany

[9]Friede Springer, Centre of Cardiovascular Prevention at Charité, Charité University Medicine Berlin, Berlin, Germany

[10]Department of Neurology, Medical Faculty, Heinrich-Heine-University, Düsseldorf, Germany

[11]Institute for Stroke and Dementia Research, Ludwig-Maximilians-University Hospital, Ludwig Maximilians University, Munich, Germany

[12]Helmholtz Munich, Research Unit for Precision Regenerative Medicine (PRM), Member of the German Center for Lung Research (DZL), Munich, Germany

[13]Institute of Experimental Pneumology, Ludwig-Maximilians University Hospital, Ludwig-Maximilians University, Munich, Germany

[14]Verna and Marrs McLean Department of Biochemistry and Molecular Pharmacology, Baylor College of Medicine, Houston, Texas, USA

[15]Therapeutic Innovation Center, Baylor College of Medicine, Houston, Texas, USA

Manuscript handled by: Shrey Kohli

Final decision: Shrey Kohli, 16 October 2024

Amin Polzin and Marcel Benkhoffcontributed equally to this study.

Correspondence
Amin Polzin, Pneumologie und Angiologie Universitätsklinikum, Düsseldorf Klinik für Kardiologie, Moorenstraße 5, Düsseldorf, 40225 Germany.
Email: amin.polzin@med.uni-duesseldorf.de

Tobias Petzold, Deutsches Herzzentrum der Charité University Hospital Berlin, Department of Cardiology, Angiology and Intensive Care Medicine, Campus Benjamin Franklin, Hindenburgdamm 30, Berlin 12203, Germany
Email: tobias.petzold@dhzc-charite.de

Funding information
This study was funded by German Research Foundation (DFG) grant No. 236177352–CCR 1116 (A.P., M.K.), grant No. 493400536 (A.P., T.P.), grant No. 413659045 (A.P.), grant No. 510844896 (A.P.), grant No 530690968 (M.B.), grant No. PE 2704/3-1 (T.P.), grant No. 541206655 (T.P.), Heisenberg Program 541206600 (T.P.). DZHK (German Center for Cardiovascular Research) grant megacariocyte project-BHF-DHF-DZHK funding scheme was granted to T.P. LMU Munich's Clinician scientist program in vascular medicine and LMU Munich's institutional Förderprogramm für Forschung und Lehre was granted to M.T. German Heart Foundation grant No. F/32/22 was granted to A.P. Medical Faculty of the Heinrich Heine University grant No. 18-2019 was granted to A.P. and grant No. 2021-01 to P.M.

Abstract

Background: Immediate activated factor (F)X (FXa) inhibition exerts direct antiplatelet effects in the context of arterial thrombosis but little is known about the impact of long-term therapy on platelet function in ischemic cardiovascular diseases.

Objectives: Therefore, we analyzed platelet-derived effects of long-term FXa inhibition in the setting of acute myocardial infarction (AMI) and stroke.

Methods: We evaluated the effect of acute versus chronic FXa inhibition on thromboinflammation following AMI and stroke in mice *in vivo*. Mechanistically, we identified changes in platelet gene expression and proteome under chronic FXa nonvitamin K antagonist oral anticoagulant treatment and characterized its functional consequence on platelet physiology. In a prospectively recruited cohort of patients with AMI, we determined cardiovascular magnetic resonance based cardiac endpoints under FXa nonvitamin K antagonist oral anticoagulant effects on clinical endpoints in a cohort of patients with AMI.

Results: Chronic but not acute FXa inhibition reduced cerebral and myocardial infarct size and improved cardiac function 24 hours after AMI in mice. Mechanistically, we identified an attenuated thromboinflammatory response with reduced neutrophil extracellular trap formation in mice and patient samples. Proteome and RNA expression analysis of FXa inhibitor treated patients revealed a reduction of key regulators within the membrane trafficking and secretion machinery hampering platelet α and dense granule release. Subsequent, thromboinflammatory neutrophil extracellular trap density in thrombi isolated from stroke and myocardial infarction patients was reduced. Patients with AMI treated with FXa inhibitors showed decreased infarct size after myocardial infarction compared to patients without anticoagulation treatment.

Conclusion: Long-term FXa inhibition induces antithromboinflammatory proteome signatures in platelets, improving infarct size after myocardial infarction and stroke.

KEYWORDS
myocardial infarction, factor Xa, platelets, thromboinflammation

1 | INTRODUCTION

Long-term oral activated factor (F)X (FXa) inhibition is a well-established therapy for the prevention of thromboembolic events and an increasing number of additional indications [1–4]. Available nonvitamin K antagonist oral anticoagulants (NOACs) show comparable efficacy with a lower rate of bleeding events [5–8]. Beyond inhibition of the plasmatic coagulation cascade by targeting FIIa (thrombin) or FXa, NOACs show noncanonical pleiotropic effects on platelet function [9]. Thereby, FIIa inhibition is associated with a prothrombogenic platelet phenotype [10,11] with mildly increased risk for myocardial infarction in patients [12]. In contrast, FXa inhibition attenuated arterial thrombosis in an experimental setting by decreasing FXa mediated PAR-1 activation on platelets [13] while reducing thrombotic events including myocardial infarction in patients [14].

Myocardial infarction and ischemic stroke are prototypic thromboinflammatory cardiovascular diseases, arising from a dysregulated interplay between the innate immune system, platelets, and the coagulation system [15]. Recently, it has been shown that chronic FXa treatment attenuated myocardial inflammation and tissue damage in a murine model of myocardial infarction [16]. Along this line, NOAC treatment reduced ischemic tissue injury in patients with recurrent stroke indicating antiinflammatory effects upon chronic treatment [17]. However, the underlying mechanism of these antithromboinflammatory effects remains insufficiently understood.

Intravascular thromboinflammation is fostered by recruited platelets driving immune cell activation by release of damage-associated molecular patterns as well as direct physical interaction [15,18,19]. Interfering with this, thromboinflammatory cellular interplay at the site of injury represents a so far clinically unutilized

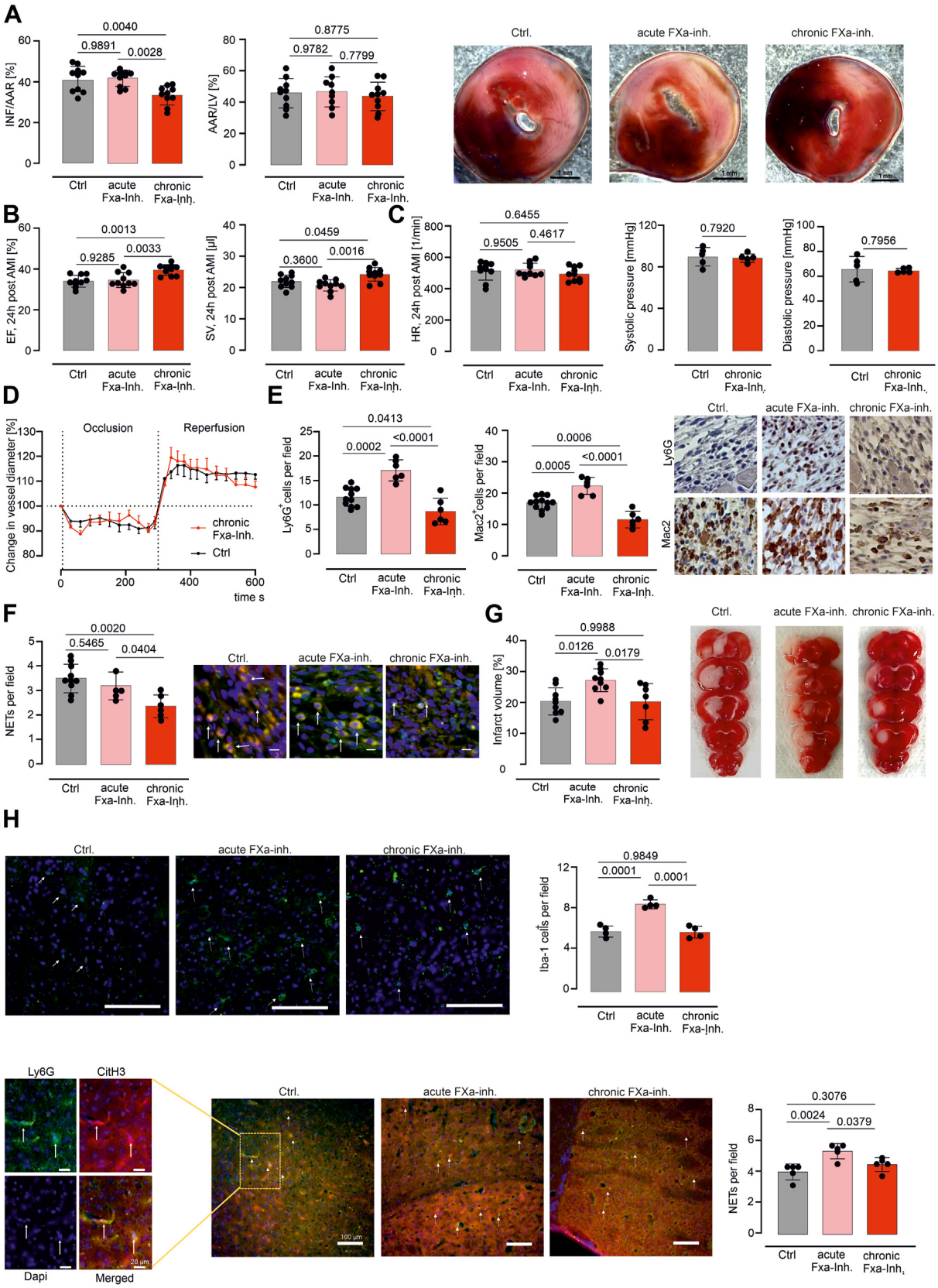

FIGURE 1 (A) Chronic oral activated factor (F)X (FXa)-inhibition prior to acute myocardial infarction (AMI) led to decreased infarct size after 24 hours of reperfusion compared to acute FXa inhibition and control treatment (one-way ANOVA, $n = 10$). Area at risk (AAR/left ventricle) did not differ between the groups. Exemplary images of TTC-stained infarct area are provided on the right side. (B) Echocardiographic assessment revealed improved cardiac function (EF = ejection fraction; SV = stroke volume) 24 hours after AMI in mice treated with FXa inhibition

therapeutic approach to improve outcomes in ischemic cardiovascular disease. In this study, we identified chronic FXa inhibition by NOACs as regulator of platelet proteome that induces an antithromboinflammatory platelet signature attenuating platelet granule secretion and subsequent thromboinflammation *in vivo* and in patients. Further, we found improved patient's infarct size in an exploratory, prospectively recruited patient cohort.

2 | RESULTS

2.1 | Chronic but not acute FXa inhibition reduces thromboinflammation and improves infarct size in murine acute myocardial infarction and stroke

To question whether chronic FXa inhibition impacts on thromboinflammation and functional outcome following myocardial infarction *in vivo*, mice were treated over 5 weeks prior to induction of acute myocardial infarction (AMI). FXa inhibitor-treated animals showed a decreased infarct size by 19% (Figure 1A) compared to acute FXa inhibition over 2 days or vehicle-treated controls. In parallel, chronically treated animals showed a functionally higher ejection fraction and stroke volume (Figure 1B) 24 hours after induction of myocardial injury. In contrast, acute FXa inhibition did neither protect from cardiac tissue damage resulting in similar large infarct size nor preserved cardiac function compared to vehicle treatment (Figure 1A, B). Of note, no effect on blood pressure or vessel diameter during flow-mediated dilatation (FMD) measurement, as a marker for endothelial function, between groups was found (Figure 1C, D). Levels of plasma FXa inhibitor were similar between acute and chronically treated animals (Supplementary Figure S1A).

To resolve the underlying mechanism of this protective effect, we found a reduced recruitment of innate immune cells (ie, $Ly6G^+$ neutrophils and $Mac2^+$ cells) in the infarcted area after 5 days by histologic assessment (Figure 1E). Along this line, we identified reduced plasma levels of some prothromboinflammatory cytokines (eg, IL-1α [20] and IL-6 [21,22]) after 24 hours, although the majority of cytokines was not affected (Supplementary Figure S1B). To more specifically assess the thromboinflammatory response within the injured tissue, we quantified neutrophil extracellular traps (NETs) and found an attenuated response under chronic but not acute FXa inhibition (Figure 1F).

To assess whether the attenuating effect of chronic FXa treatment on thromboinflammation extends to another disease entity, we investigated an ischemic stroke model (transient middle cerebral artery occlusion [tMCAO]) model. Chronic FXa inhibition led to 25% smaller brain infarct volume 24 hours after stroke compared to mice treated over 2 days (Figure 1G). Chronically treated mice showed reduced numbers of Iba-1 positive cells, representing activated microglia and macrophages. Further, we found a reduced number of NETs 24 hours after tMCAO as compared to acute treatment (Figure 1H). Flow cytometry analysis of infarcted brains showed a reduced number of microglia but not neutrophils in mice with chronic FXa inhibition (Supplementary Figure S2A). Subsequent, RNA expression based analysis of tissue inflammation did not show alteration between the chronic and acute FXa inhibition (Supplementary Figure S2B).

2.2 | Infarct size reduction of chronic FXa inhibition is platelet-dependent

To elucidate whether chronic FXa inhibition also affects the thromboinflammatory response within intravascular formed thrombi, we analyzed mechanically recovered thrombus material from patients with cardioembolic stroke under FXa therapy (Supplementary Table S1). Again, chronic FXa inhibition associated with reduced intravascular NET formation, indicating that chronic FXa inhibition attenuated the thromboinflammatory response (Figure 2A). Platelet-driven neutrophil activation is a key trigger for NET formation in the context of cardiovascular thromboinflammation following ischemic tissue injury [23]. Thus, to investigate whether chronic FXa treatment affects platelet induced NET formation, we established a platelet-neutrophil coculture model from patients under chronic FXa treatment (Supplementary Table S2). Following platelet stimulation with thrombin and collagen, we observed a reduced NET formation while PMA (Phorbol-12-myristat-13-acetat; 50 nM) induced NET formation in sole neutrophil cultures from the same individual were unaffected (Figure 2B). These data indicate that observed

chronically (one-way ANOVA, $n = 10$). (C) Heart rate in echocardiographic assessment did not differ between the groups (one-way ANOVA, $n = 10$). The measurement with Millar catheter showed that neither systolic nor diastolic blood pressure changed due to chronic oral FXa inhibition (unpaired t-test, $n = 5$). (D) Flow-mediated dilation expressed in change in vessel diameter [%] revealed no difference in endothelial function between mice with chronic oral FXa inhibition and control mice (unpaired t-test, $n_{Ctrl} = 9$, $n_{chronic\ FXa\text{-}Inh.} = 5$). (E) Accumulation of neutrophils ($Ly6G^+$ cells) in the infarcted area 5 days after AMI was increased in mice with acute FXa inhibition compared to control mice. Chronic application of FXa inhibition, on the contrary, led to reduced accumulation of neutrophils compared to control mice (one-way ANOVA, $n_{Ctrl} = 11$; $n_{FXa\text{-}Inh.} = 6$). The accumulation of macrophages ($Mac2^+$ cells) 5 days after AMI behaves in the same way (ANOVA analysis, $n_{Ctrl} = 11$; $n_{FXa\text{-}Inh.} = 6$). Exemplary images (100 × 100μm) of Ly6G- and MaC2- staining can be found next to the graphs. (F) Occurrence of NETosis ($Ly6g^+/H3^+$) was reduced in mice with chronic treatment but not in mice with acute treatment (one-way ANOVA, $n_{Ctrl} = 10$; $n_{FXa\text{-}Inh.} = 6$). Exemplary images (scale bar 10μm) are provided. (G) Acute oral FXa inhibition prior transient middle cerebral artery occlusion led to increased brain infarct size after 24 hours of reperfusion compared to chronic FXa inhibition and control treatment (one-way ANOVA, $n_{Ctrl} = 9$; $n_{acute\ FXa\text{-}Inh.} = 9$, $n_{chronic\ FXa\text{-}Inh.} = 7$). Images of TTC-stained brains can be found on the right. (H) This higher infarct size led to higher accumulation of activated microglia (Iba-1^+ cells) and higher occurrence of NETosis ($Ly6g^+/H3^+$) 24 hours after transient middle cerebral artery occlusion (one-way ANOVA, $n = 5$). Exemplary images (scale bar 100μm) can be found on the left. Data shown as mean ± SD. ANOVA, analysis of variance; AMI, acute myocardial infarction; NETosis, neutrophil extracellular trap formation; TTC, 2,3,5-Triphenyl-tetrazolium chloride.

antithromboinflammatory effects under chronic FXa inhibition are platelet derived. To test this hypothesis *in vivo*, we repeated AMI experiments under thrombopenic conditions in chronic and control-treated animals. Histologic and functional assessment of cardiac function revealed that antibody-mediated platelet depletion showed no additional protective effect of chronic FXa inhibition, yielding larger infarct size and reduced cardiac function (Figure 2C, D).

2.3 | FXa inhibition alters platelet RNA and protein expression

Having identified platelets as mediators of the antithromboinflammatory effect under chronic FXa treatment, we aimed to access the underlying mechanism. Therefore, we addressed the effect of chronic FXa inhibition on platelet RNA and proteome expression. For this, we analyzed individuals taking NOACs for the prevention of thromboembolic events as the largest patient cohort under chronic therapy. We serially analyzed platelet samples from patients undergoing ablation for atrial flutter receiving chronic anticoagulation with FXa inhibitors postinterventional for 4 to 6 weeks (time point 1, under FXa inhibition) and 4 weeks after stopping intake due to sustained sinus rhythm in clinical follow-up (time point 2, after stopping; Supplementary Table S3). Unsupervised dimension reduction using principal component analysis separated treated from control samples, indicating that the treatment induced global changes in both RNA and proteome levels (Figure 3A, B). Independent differential expression analyses revealed 1081 and 44 genes with significantly altered RNA and protein abundance, respectively (false discovery rate [FDR] < 0.05). Integrated differential expression revealed 29 genes that showed concomitant regulation on both gene and protein levels after stopping FXa inhibitor treatment. Gene set enrichment analysis of this set of genes revealed membrane trafficking and vesicle-mediated transport as the most significantly regulated terms under chronic FXa intake (Figure 3C). To verify our findings on a single gene level, we analyzed VAMP-8 and found a concomitant downregulation of RNA and protein levels (Figure 3D). In line with this, we found significant downregulation of VAMP-8 in platelets from patients treated with FXa antagonist when compared to untreated controls, using immunoblotting (Figure 3E).

2.4 | Reduced platelet secretion under chronic FXa inhibition attenuates thromboinflammation

Given that platelet granule secretion is a critical step to drive NET formation, we questioned whether downregulation of the secretion machinery under chronic FXa inhibition attenuates platelet granule release. Investigating serotonin release upon platelet stimulation, we observed an impaired release from dense granules (δ-granules), although washed platelet aggregation is not altered [13] (Figure 4A, B). Concomitantly, we found elevated residual levels of α-granules stored von Willebrand factor (VWF) in platelets following stimulation (Figure 4C), indicating an attenuated cargo protein release. To further investigate alteration in vesicle trafficking we quantified the distribution of VWF-positive granules within the platelet and observed a reduced dislocation to the outer parts of the cell (Figure 4D), indicative of an altered vesicle handling by platelet under chronic FXa inhibition.

2.5 | Patients treated with FXa inhibitors showed decreased infarct size after AMI

Having identified chronic FXa inhibition as a regulator of platelet proteome that attenuates platelet-driven thromboinflammation, we questioned its relevance in patients presenting with AMI. In an exploratory, prospective, monocentric, and translational study, we analyzed 335 patients with ST-elevation myocardial infarction (STEMI) who underwent cardiovascular magnetic resonance (CMR) imaging (Figure 5A) for quantification of infarct size and myocardial edema 5 days after STEMI. One hundred thirty-three patients were excluded from analysis as shown in the flowchart (Figure 5B). From 202 patients entering the subsequent analysis, 29 patients were treated with FXa inhibitors and underwent inverse probability treatment weighting (IPTW, propensity score, Supplementary Table S4) to adjust for differences in baseline characteristics between groups (Supplementary Table S5). After weighting, both groups were similar regarding characteristics, procedural details, comorbidities, and medication. CMR endpoint analysis revealed that FXa inhibitor-treated patients exhibited reduced infarct size and myocardial edema 5 days after STEMI compared to patients without oral anticoagulation (Figure 5 C, D). Platelet reactivity was not altered between the groups (Supplementary Table S5). These data indicate that the attenuated platelet-driven thromboinflammation under chronic FXa inhibition, may improve the patient's outcome. An overview of all cohorts used in this article is provided (Supplementary Figure S3).

3 | DISCUSSION

In this study, we uncovered a novel platelet-derived antithromboinflammatory effect of long-term FXa inhibition. The main findings of this study are: (1) chronic FXa inhibition improves infarct size after experimental AMI and stroke as compared to acute FXa inhibition. (2) As underlying mechanism, we identified attenuated platelet-driven thromboinflammation and NET formation under chronic FXa inhibition. (3) Chronic FXa inhibition downregulates cellular pathways involved in platelet degranulation. (4) Chronic FXa inhibition reduces infarct sizes in a prospectively collected AMI patient cohort.

Chronic oral FXa inhibition is a well-established therapy for the prevention of thromboembolic events and an increasing number of additional indications [1–4]. Numerous studies showed comparable efficacy combined with a lower risk of bleeding events when compared to VKA. Beyond its efficient and safe anticoagulative mode of action, we have earlier identified pleiotropic antithrombotic effects

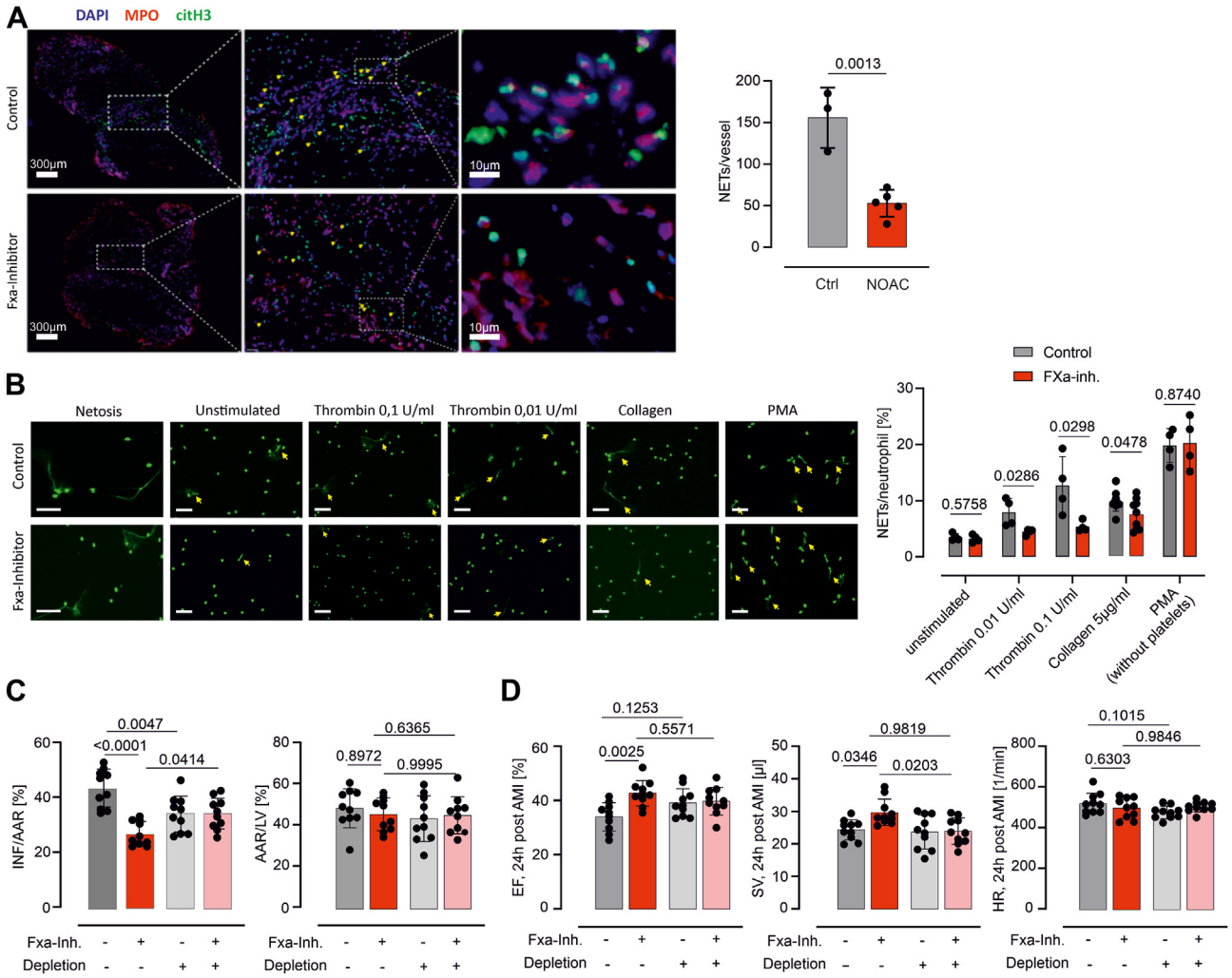

FIGURE 2 (A) Neutrophil extracellular traps (NETs) in recovered thrombi from patients with acute stroke were analyzed with confocal microscopy. Scale bar represents 500 µm. Magnifications of thrombus areas with NET structures [MPO- 4′,6-diamidino-2-phenylindole (DAPI) -CitH3 triple positive cells] are shown on the right. Quantitative comparison of NETs per vessel is shown as a bar plot on the right (n = 3 for control, n = 5 for activated factor [F]X FXa inhibition). (B) Quantification of NETs per neutrophil in humans under FXa inhibition after stimulation of platelets with the indicated agonists (n = 4 for unstimulated, thrombin and PMA; n = 10 for control collagen 5 µg/mL; n = 9 for FXa inhibitor collagen 5 µg/mL). Scale bar represents 10 µm; magnification of NET structure is shown on the left. (C) The infarct size decreasing effect of chronic oral FXa inhibition is abolished in platelet depleted mice (two-way ANOVA, n = 10). Area at risk (AAR/left ventricle) did not differ between the groups. (D) An improvement in cardiac function (HR = heart rate; EF = ejection fraction; SV = stroke volume) 24 hours after acute myocardial infarction of chronic oral FXa inhibition can also no longer be detected in platelet depleted mice (two-way ANOVA, n = 10). Data shown as mean ± SD. NET, neutrophil extracellular trap.

on platelet function. While this effect depends on the inhibition of FXa-induced platelet activation via PAR-1 attenuating platelet adhesion and thrombus formation [13], little mechanistic insight exists on FXa-mediated long-term effects.

Some studies describe an improvement in outcome after AMI under chronic FXa inhibition [16,24], although the tissue protective effect was attributed to a local attenuation of the inflammasome as well as some systemic inflammation [25–28]. A recently published study demonstrated that FXa inhibition attenuates neutrophil maturation in the bone marrow leading to reduced immune response after AMI [29]. Indeed, we did not see a clear effect on systemic inflammation by FXa inhibition in our study, which may be due to different dosages as we chose the lowest dose of rivaroxaban that inhibits FX activity in mice [16].

Beyond their central role in primary hemostasis and pathogenesis of acute atherothrombosis, platelets contribute to the maintenance of vascular integrity, defense mechanisms of the innate and adaptive immune system [30] as well as tissue regeneration in the context of AMI or stroke [31,32]. The platelet secretome consists of a plethora of bioactive substances [33–39] stored in α- and δ-granules [40], which is of particular importance in this context. In line with this, genetic inhibition of δ- or α-granule secretion resulted in smaller infarct volumes after ischemic stroke, although a simultaneous inhibition of both drastically hampers hemostasis increasing secondary hemorrhage [18]. Our findings emphasize that granule secretion is critical for thromboinflammatory NET formation [19,20] which is associated with patients' outcomes after stroke and AMI [23,41].

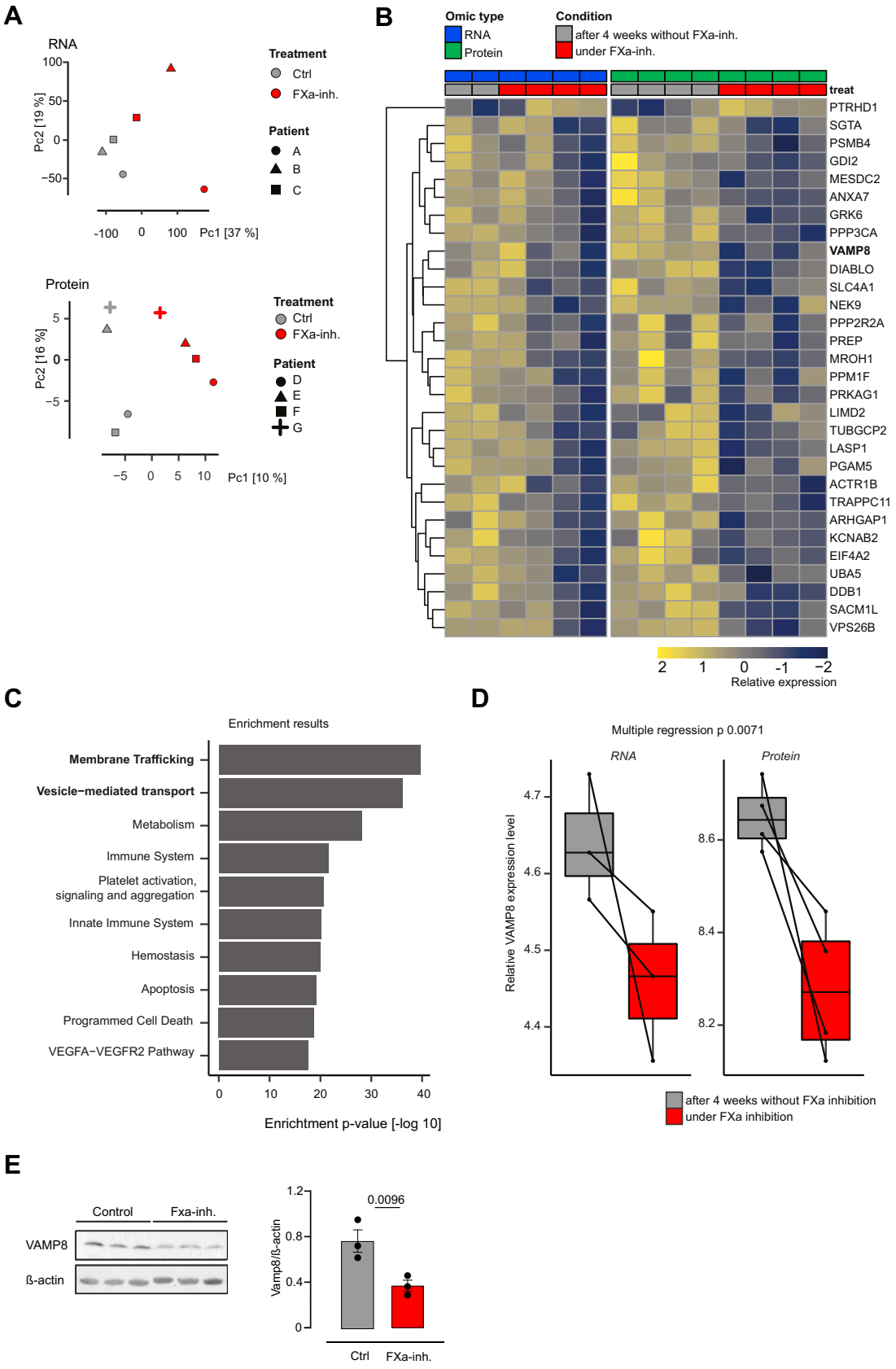

FIGURE 3 Platelet RNA and proteome expression was serially analyzed in samples from patients undergoing ablation for atrial flutter receiving a chronic anticoagulation with FXa inhibitors post interventional for 4 to 6 weeks (time point 1, under activated factor [F]X FXa inhibition) and 4 weeks after stopping intake due to sustained sinus rhythm in clinical follow-up (time point 2, after stopping). (A) Principal component analysis separates treated from control samples based on RNA (top) and protein expression (bottom). (B) Heatmap illustrates genes

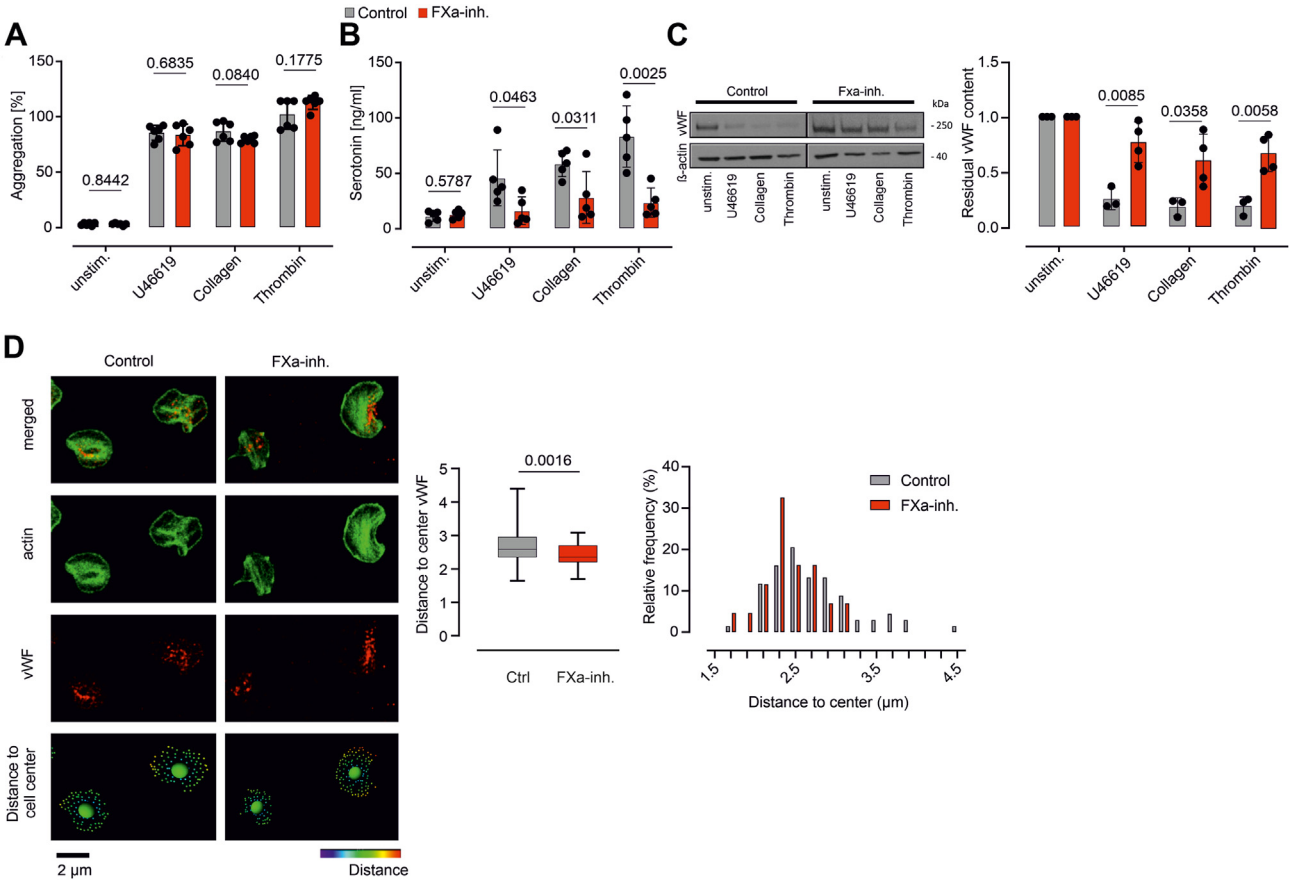

FIGURE 4 (A) Light transmission aggregometry of washed platelets form patients with or without activated factor (F)X (FXa) therapy due to atrial fibrillation was assessed after stimulation with the indicated agonists (n = 6). (B) Serotonin level in supernatant after platelet stimulation with the indicated agonists. (C) Residual VWF contents in platelets after stimulation with the indicated agonists. Representative immunoblot is shown. D) Analysis of VWF positive membrane compartment (vesicles) in patients under chronic oral FXa inhibition and healthy controls (n = 4 per group). Representative immunofluorescence images of thrombin-stimulated platelets (red: VWF, green: phalloidin are shown, scale corresponds to 2 µm. Quantification of the mean vesicle distance to the calculated cell centre (middle). Distance distribution histogram of VWF positive vesicles within the cell. Symbols represent individual cells (right). Data shown as mean ± SD. VWF, von Willebrand factor.

Several studies revealed a pleiotropic antiinflammatory effect of FXa inhibition [42,43]. In contrast, in our experiments, acute treatment suggests a proinflammatory response at first sight. However, we interpret our data on the murine experiments to mean that acute treatment has not yet achieved any coagulation-independent antiinflammatory or antithromboinflammatory efficacy. The changes we have described that are required for this (platelet proteome alteration) do not yet exist at this time. Due to the already effective anticoagulation, there is increased bleeding in the tissue. This leads to an increased number of inflammatory cells and increased thromboinflammation in the tissue. In the heart, a change in the immigrated immune cells can be seen, but no change in the size of the infarct. As the brain is significantly more sensitive, increased bleeding under anticoagulation in this model leads to an increased infarct size [44]. In contrast, chronic treatment shows the full antithromboinflammatory effects and leads to reduced infarct size in both models compared to acutely treated animals.

In our study, FXa inhibition interferes with granule release by downregulation of central proteins within vesicle trafficking and secretion proteins on gene expression and protein level. Among the genes most markedly regulated once was VAMP-8, which is an important component of the granule secretion machinery for α- and δ-granules release [45–47]. Thus, our data show that FXa inhibition interferes with granule functionality in platelets. Though the underlying mechanism of protein regulation in platelets under FXa inhibition remains to be elucidated, our data suggest that changes in gene

with concordant differential expression between treated and control samples across both proteome and RNA profiles. (C) GO enrichment analysis was performed only for genes that showed downregulation at both the RNA and protein levels. Indication of the most upregulated signaling pathways under FXa inhibition. (D) For example, VAMP-8 was downregulated under direct FXa inhibition at the RNA (left) and protein (right) level. Data sets shown were generated from 3 and 4 patients for RNA and proteome, respectively, under or after discontinuation of oral FXa inhibition; significance levels (P values) are indicated. (E) VAMP-8 content in platelets of FXa inhibitor treated patients or healthy controls assessed by immunoblotting (n = 3).

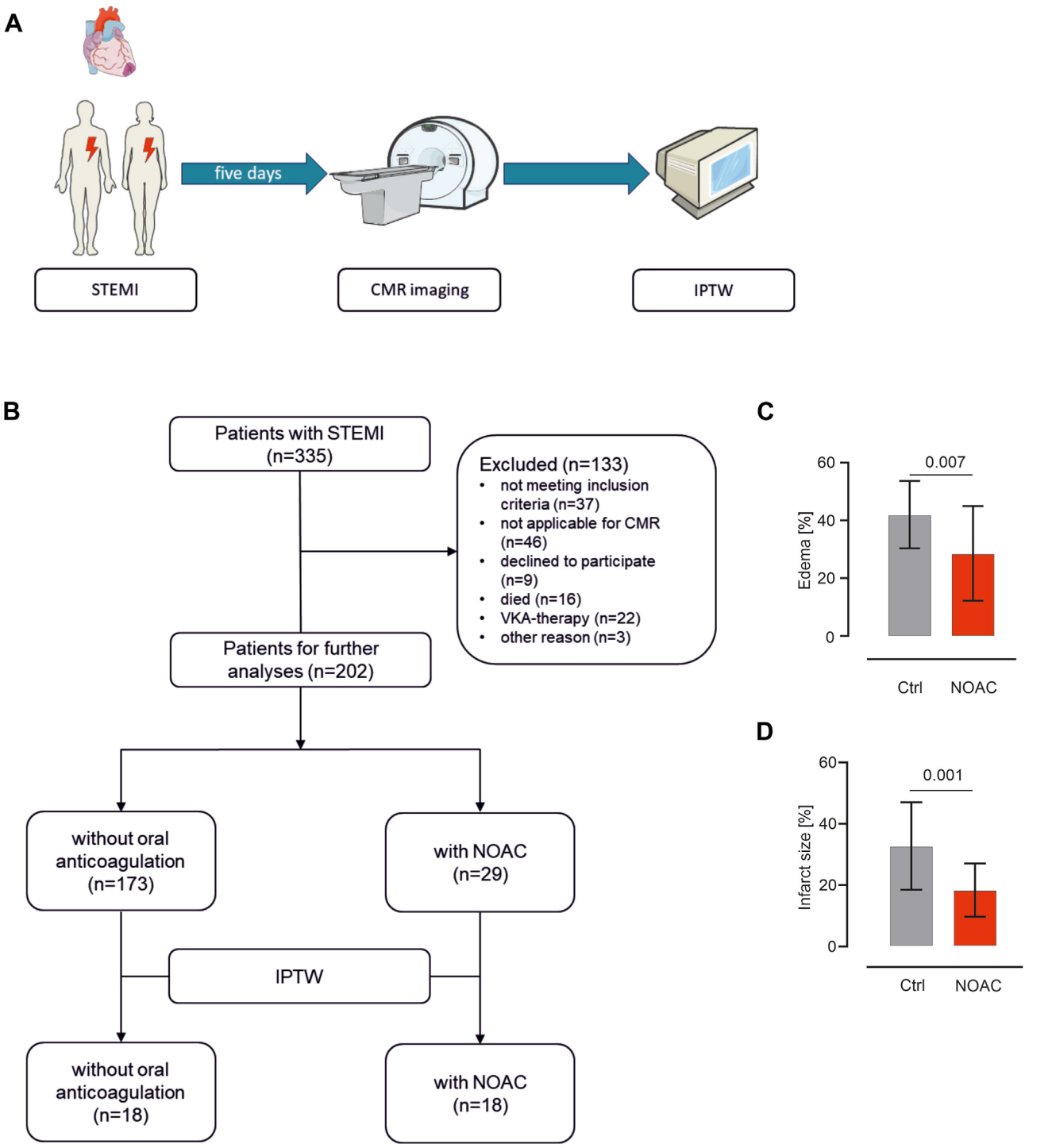

FIGURE 5 (A) Study protocol: 5 days after ST-elevation myocardial infarction, patients underwent cardiac magnet resonance imaging to detect infarct size and edema in myocardium. Afterward, inverse probability treatment weighting (propensity score) was used to analysis NOAC effects. Exemplary images of cardiac magnet resonance images can be found on the right. (B) Flow chart of study procedure. (C) Patients already treated with NOAC showed reduction in edema 5 days after ST-elevation myocardial infarction compared to patients without oral anticoagulation (n = 18). (D) Infarct size was also decreased in NOAC treated patients (n = 18). Parts of the figure were drawn by using pictures from Servier Medical Art. Servier Medical Art by Servier is licensed under a Creative Commons Attribution 3.0 Unported License. Data shown as mean ± SD. NOAC, nonvitamin K antagonist oral anticoagulant.

expression arise on the platelet progenitor, the megakaryocyte, level within the bone marrow.

In summary, our study reveals previously unknown thromboprotective mechanisms of FXa inhibition by attenuating deleterious thromboinflammation in the context of common ischemic cardiovascular diseases. Thus, future studies will have to delineate the dose dependency of these effects under chronic therapy in the clinical setting. Against the background of earlier published literature, our

findings provide an additional platelet-dependent protective mechanism that may further improve primary and secondary prevention in patients with thromboinflammatory cardiovascular disease including coronary artery disease and stroke.

4 | CONCLUSION

We revealed a coagulation-independent mechanism of FXa inhibitors, attenuating platelet-driven thromboinflammation and improving patient infarct size and improved cardiac function following myocardial infarction. Hence, our data provide evidence that NOACs may be used for secondary prevention in patients with thromboinflammatory diseases.

5 | LIMITATIONS

This study has several limitations. The sample size in some analyses is small, but statistically significant results could still be obtained. Acute FXa treatment showed different results in tMCAO and AMI models compared with untreated controls. However, the comparison between acute vs chronic treatment has very similar results regardless of the model. Most patients are treated with apixaban which has prevailed clinically over other FXa inhibitors just in recent years due to its low bleeding complications [48], not rivaroxaban as in the mouse model. Nevertheless, we do not expect any differences in VAMP inhibition assuming a group-specific mechanism here [49]. Furthermore, a selection bias cannot be ruled out completely, as 133 out of 355 patients had to be excluded from further analysis. Nevertheless, the number of patients for this exploratory study is large enough for a meaningful analysis to be performed by IPTW. The nature of this study is to identify a new and previously unknown platelet-depended mechanism of FXa inhibition. Of note, all patients included in this study received full-dose anticoagulation for stroke prevention in atrial fibrillation or flutter. According to the manufacturer's information and based on current guidelines, the FXa inhibitor doses administered were adjusted by the treating physicians to the age, weight, and kidney function of the individual patient. Consequently, different doses of FXa inhibitor were administered, nevertheless, it corresponded to full anticoagulation in each of these patients. However, a dose dependency cannot be excluded and will be worked out in larger studies in the future.

6 | METHODS

6.1 | Animals

C57Bl/6J mice were purchased at the age of 12 to 15 weeks from Janvier Labs (Saint-Berthevin). All animals had free access to normal chow and drinking water. The light conditions in the housing of the mice were based on a 12-hour day and night rhythm. Mice were randomly divided into control and treatment groups. The animals were not operated and analyzed in blocks, but in a random order to minimize possible confounders. Investigators were blinded. An *a priori* sample size calculation could not be performed due to the pilot nature of the study. All experiments were approved by *Landesamt für Natur, Umwelt und Verbraucherschutz Nordrhein-Westfalen* (LANUV, 81-02.04.2021.A001) and in accordance with the European Convention for the Protection of Vertebrate Animals used for Experimental and other Scientific Purposes (Council of Europe Treaty Series No. 123) and 2010/63/EU. We used the ARRIVE checklist when writing our report [50].

6.2 | Treatment of FXa inhibitor

Mice were randomly divided into treatment and control groups. Chronic FXa inhibition was performed with rivaroxaban (RIVA) treatment for 5 weeks. For this, RIVA (ApexBio) was dissolved in phosphate-buffered saline (PBS) and administered every 2 days at a dose of 3 mg/kg body weight by oral gavage [51]. As a linear murine dose–response relationship of RIVA with respect to prothrombin time and anti-FXa activity has already been described [52], we chose a low dose that would guarantee us a still present inhibition of FX activity and at the same time be as low as possible to reflect the human situation [25]. Acute treatment was given at the same dosage for 2 days. Animals from the control group received PBS at the identical interval.

6.3 | Murine model of AMI

Mice underwent ischemia/reperfusion surgery as a murine model of AMI, as previously described [53]. Briefly, after intubation of the mice, surgery was conducted under isoflurane anesthesia (2 vol %). Afterward, AMI was initiated via temporary left anterior descending artery ligation for 30 minutes. Body temperature and typical ST-elevations in electrocardiogram were monitored continuously during the entire procedure. This open-chest surgery was followed by 24 hours and 5 days of reperfusion, respectively. To reduce pain, mice were treated with buprenorphine (0.1 mg/kg, Temgesic, Indivior) for up to 3 days. Platelet depleted mice are not eligible for open-chest murine model of AMI due to bleeding complications. Therefore, a closed-chest model of AMI was used with these mice. Detailed information is provided in supplemental material.

6.4 | Echocardiographic assessment of murine cardiac function

Cardiac function was assessed 24 hours before and 24 hours after induction of AMI by echocardiography as described before [54]. Briefly, mice were anesthetized with isoflurane (2 vol%) and their body temperature was kept between 37 °C and 38 °C. Left ventricular functional parameters were measured with high resolution 18 to 38 MHz ultrasound transducer (MS 400, VEVO 3100, Visual Sonics Inc).

Post processing analyses were performed offline using commercial software (VevoLab 3.2.6., Visual Sonics Inc).

6.5 | Measurement of arterial blood pressure

Measurement of arterial blood pressure in mice was conducted with 1.4F Micro-Tip catheter transducer (Millar Inc) as previously described [55]. Briefly, catheter transducer was inserted into the aorta of anesthetized mice (isoflurane, 2 vol %) via arteria carotis communis. Body temperature was kept between 37 °C and 38 °C. The pressure data were obtained with the help of the software IOX (v 2.4.5.6, emka technologies, Falls Church).

6.6 | FMD

FMD was measured in isoflurane-anesthetized mice as described previously [56,57]. Briefly, a loop occlude was positioned upstream of the femoral artery. The artery was occluded for 5 minutes which was followed by 5 minutes of reperfusion. The diameter of the femoral artery was measured via a 30 to 70 MHz ultrasound transducer (MS 700, VEVO 3100, Visual Sonics Inc). Post processing analyses were performed offline using commercial software (VevoLab 3.2.6., Visual Sonics Inc). Diastolic vessel diameters are presented in percent of baseline.

6.7 | Myocardial infarct size measurement

Mice were first anesthetized with ketamine (100 mg/kg body weight, Ketanest, Zoetis) and xylazine (10 mg/kg body weight, Rompun, Bayer AG) by intraperitoneal injection and then sacrificed 24 hours after induction of AMI. Hearts were taken out of the sacrificed mice, surrounding tissue was removed, and hearts were flushed with cold saline solution via aorta to remove blood. Next, ligation of left anterior descending artery was repeated in a permanent manner. Afterward, the hearts were perfused with 1% Evans blue dye (Sigma Aldrich), which separates nonischemic myocardium from area at risk (AAR). Hearts were frozen at −20 °C overnight and then cut into six 1-mm slices starting apical. The slices were incubated for 5 minutes with 1% TTC solution (2,3,5-Triphenyl-tetrazolium chloride, Sigma Aldrich), which colors vital tissue. Infarct size/AAR-ratio and AAR/left ventricle-ratio were determined via computer-assisted planimetry.

6.8 | Murine inflammation panel assay

Inflammatory cytokines in plasma were measured 24 hours post AMI. Therefore, LEGENDplex Mouse Inflammation Panel (Biolegend) was performed according to the manufacturer's instructions.

6.9 | Assessment of rivaroxaban plasma level

Plasma levels of rivaroxaban in mice were determined by anti-FXa-activity measurement according to manufacturer's instructions (Biophen, Hyphen BioMed).

6.10 | tMCAO

Mice underwent tMCAO surgery as a murine model of stroke as previously described [58]. Briefly for transient occlusion of the middle cerebral artery a silicon-coated thread (6-0 medium MCAO suture L910 PK10, Doccol corporation) was inserted through the right internal carotid artery. After staying in the middle cerebral artery for 60 minutes, thread was removed to guarantee reperfusion. To quantify infarct volume animals were anesthetized with ketamine (100 mg/kg body weight, Ketanest, Zoetis) and xylazine (10 mg/kg body weight, Rompun, Bayer) by intraperitoneal injection and decapitated 24 hours after tMCAO. Afterward, brains were removed and cut into 2-mm coronal sections which were stained in 1% TTC solution. Infarct volume was determined via computer-assisted planimetry. Infarcted brains were also analyzed via flow cytometry and real time polymerase chain reaction. Detailed information on this can be found in Supplementary Material on pages 3/4.

6.11 | Immunohistochemical staining and quantification

Detailed information about histologic assessment of murine hearts and brains are provided in Supplementary Material on pages 1–3.

6.12 | STEMI patients and study design

We performed a prospective, explorative, monocentric, and translational study in 335 patients with STEMI. Patients with coagulopathies and malignant comorbidities with a life expectancy of less than 1 year were excluded from further analyses. Written informed consent was obtained from all participants. To determine infarct size, gadolinium-based contrast agent (Gadovist, Bayer Healthcare, 0.2 mmol/kg) was used to detect late gadolinium enhancement in cardiac magnet resonance imaging 5 days after STEMI during clinical follow-up [59,60]. Post processing analyses were performed offline using commercial software (cmr42, Circle Cardiovascular Imaging Inc and Extended Workspace, Philips Healthcare). Infarct size and edema were determined in percent from myocardium. Experienced cardiologist regarding CMR-imaging performed evaluation of CMR. The study is registered under clinicaltrails.org with the ID "NCT03539133."

6.13 | Recruitment of patients under chronic FXa inhibition and blood sampling

The study conformed to the 1975 Declaration of Helsinki and was approved by the Ethics Committee of the Ludwig-Maximilians-University (LMU), Munich, and Heinrich-Heine-University, Düsseldorf. In an open, prospective design, patients with chronic FXa inhibition with rivaroxaban or apixaban due to atrial fibrillation were recruited. Exclusion criteria were known hematologic disorders, active hematologic malignancy, severe renal insufficiency with dialysis, age below 18 years. Blood from patients was obtained by venous puncture from a dorsum manus or cubital vein. A 21-G butterfly needle (Safety Multifly-Needle, Sarstedt) was used. Samples were collected in 2.9-mL 0.1 M sodium citrate tubes and 2.6-mL EDTA tubes (S-Monovette, Sarstedt).

6.14 | Recruitment of patients under temporary FXa inhibition and blood sampling

The study conformed to the 1975 Declaration of Helsinki and was approved by the Ethics Committee of the LMU. In an open, prospective design, patients undergoing ablation for atrial flutter were recruited at the LMU hospital. These patients received a temporary anticoagulation with FXa inhibitors postablation for 4 to 6 weeks (time point 1, under FXa inhibition) and after stopping intake due to sustained sinus rhythm in clinical follow-up (time point 2, without FXa inhibition). Exclusion criteria were known hematologic disorders, active hematologic malignancy, severe renal insufficiency with dialysis, age below 18 years. Blood from patients was obtained by venous puncture from a dorsum manus or cubital vein. A 21-G butterfly needle (Safety Multifly-Needle, Sarstedt) was used. Samples were collected in 2.9-ml 0.1 M sodium citrate tubes and 2.6-mL EDTA tubes (S-Monovette, Sarstedt).

6.15 | Platelet isolation in humans

Citrate anticoagulated blood was centrifuged with 90 $\times g$ for 20 minutes at room temperature. Platelet-rich plasma was then diluted 1:10 in modified Tyrode's buffer (137 mM NaCl, 2.8 mM KCl, 12 mM $NaHCO_3$, 5.5 mM glucose, 10 mM HEPES, pH = 6.5) substituted with prostaglandine (PGI2, 500 ng/mL final concentration, Abcam). Platelet-rich plasma was centrifuged at 450 $\times g$ for 10 minutes at room temperature. Cells were resuspended in Tyrode's buffer (pH = 7.4). For proteome analysis, platelets were purified using a magnetic activated cell sorting (MACS) based negative isolation kit. Platelet suspension was incubated with glycophorin A MicroBeads (130-050-501, MACS Miltenyi Biotec) and CD45 MicroBeads (MACS Miltenyi Biotec) before running over a LS Column (MACS Miltenyi Biotec). Cells were pelleted at 2500 $\times g$ for 5 minutes, resuspended in lysis buffer (preOmics) and immediately frozen in liquid nitrogen.

6.16 | Mass spectrometry

The pellet cells were processed according to manufactures recommendations. Peptides from LysC and trypsin proteolysis (enzyme/protein ratio 1:100) over night at 37 °C, were purified according to the PreOmics iST protocol (www.preomics.com). Data was acquired on a Quadrupole/Orbitrap type Mass Spectrometer (Q-Exactive HF, Thermo Scientific) with a 60 minute gradient, as previously described [61]. MS raw files were subject of label free protein quantification done with the MaxQuant software [62].

6.17 | Bulk RNA sequencing

RNA was isolated from pelleted cells using the RNeasy Mini Kit (Qiagen) according to the manufacturer's recommendations. The RNA isolate was thereafter enriched for poly-A templates and submitted for whole mRNA sequencing on the Illumina HiSeq4000.

6.18 | Human neutrophil isolation

Neutrophils were isolated from whole blood using the MACS neutrophil isolation kit (Miltenyi Biotec). Briefly, whole blood was incubated with MACS negative selection antibody panel and subsequently inserted into a magnet in a fluorescence-activated cell sorting tube (StemCell Technologies). The supernatant was collected, then centrifuged at 350 $\times g$ for 7 minutes at 4° C, and the erythrocytes were consequently removed by addition of erylysis buffer (155 mM NH_4Cl, 10mM $KHCO_3$, 0.1 mM EDTA, pH 7.3). Lysis was stopped after 10 minutes by addition of PBS containing 2 mM EDTA. Isolated neutrophils were pelleted by centrifugation at 350 $\times g$ for 7 minutes at 4 °C and resuspended in PBS.

6.19 | Platelet assays

We conducted light transmission aggregometry and serotonin release assay on human platelets. In addition, we analyzed VAMP-8 content, VWF content, and platelet granule distribution. Methodological details are provided in Supplementary Material on pages 4/5.

6.20 | NET formation in platelet-neutrophil coculture

Thrombin (0.1 U/mL and 0.01 U/mL) or collagen (5 μg/mL) preactivated platelets were seeded on poly-L-lysine (Sigma Aldrich) coated coverslips. After 15 minutes, neutrophils were added and incubated for 1 hour at 37 °C. For NET formation in neutrophils alone without platelets, neutrophils were stimulated with PMA and seeded on poly-L-lysine coated coverslips. After 1 hour of incubation, cells were fixed with 4% paraformaldehyde, permeabilized (0.5% Triton

X-100) and stained with SytoxGreen (Thermo Fisher Scientific, S7020, 500 nM final concentration) and Hoechst dye (Hoechst 33342, Invitrogen). Cells were visualized by immunofluorescence microscopy (4 fields of 20 times enlarged). NETs were defined as SytoxGreen positive extracellular structures. NET forming neutrophils are shown as percentage of all neutrophils.

6.21 | Histologic analysis of human thrombi after acute stroke

To analyze the histologic structure of intravascular thrombi, we examined mechanically recovered thrombus material from patients with cardioembolic stroke under FXa therapy that were provided by the neurological faculty of the LMU, Munich. The study conformed to the 1975 Declaration of Helsinki and was approved by the Ethics Committee of the LMU, Munich. Immunofluorescent stains were prepared using a triple stain against myeloperoxidase (MPO, R&D Systems), citrullinated histone 3 (rabbit polyclonal to Histone H3, Abcam), and Hoechst (1:1000, Invitrogen). NETing neutrophils were designated as such when a triple positive staining occurred.

6.22 | Bioinformatics

Raw RNA sequencing reads were mapped to human reference genome (GRCH38.p7) using the CLC Genomics Workbench. Differential expression was performed using the limma R package [63]. For the proteome data, missing values were imputed using the missForest R package [64]. Imputed proteome expression was subjected to differential expression analysis using the limma R package. Integrated RNA and proteome expression analysis was performed in the following manner. Expression values for RNA and proteome were z-score transformed independently and subsequently merged into a single data matrix. Using the R package lme4 [65] a mixed model with the patient variable as random effect was applied to test the association between treatment and normalized expression. The R package lmerTest [66] was used to assess statistical significance of each gene and derived *P* values were corrected using FDR as implemented in the p.adjust R function. A positive coefficient indicated increased expression before compared to after treatment. Genes with FDR values less than 0.05 were considered statistically significant. Gene set enrichment analysis was performed using the enrichR R package [67]. All genes with a positive coefficient in the integrated model were subjected to enrichment analysis using the "Reactome_2016" data base as reference.

6.23 | Statistics

For statistical analyses, IBM SPSS Software and GraphPad-Prism statistical software (GraphPad software Inc) were used. Normality of distribution was tested with Kolmogorov–Smirnov test, D'Agostino-Pearson test, qq-plots, and histograms in dependence on the nature of the variables. Normally distributed continues variables were analyzed using t-test; non-normally distributed variables using Mann–Whitney U-test. Homogeneity of variance was tested with Levene test. In case of heteroscedastic data, Welch test was performed. Comparison of 3 or more groups was performed using ANOVA. If the assumption of homogeneity of variances was not met, indicated by a significant Levene test, a Kruskal–Wallis test was performed. Tukey correction was applied in multiple testing. R was required for mixed-effects analyses and adjustment for multiplicity. *P* values $< .05$ were considered significant.

ACKNOWLEDGMENTS

We acknowledge the support of the Susanne-Bunnenberg-Stiftung at the Düsseldorf Heart Center.

AUTHOR CONTRIBUTIONS

A.P., M.B., M.T., and T.P. designed the study, analyzed and interpreted data, and wrote the manuscript with the input of S.G.M., T.Z., C.M., H.B.S., L.S., S.M., and M.K. K.S., C.H., V.E., F.V.W., S.A., S.Z., D.M., E.L., J.S., S.T., M.C., M.G., and T.R. performed the human studies and statistical analysis. M.Ba., P.M., Z.Z., S.C., L.W., G.A.K., A.U., H.H., L.V., A.T., S.P., and G.P. collected and analyzed murine data and revised the manuscript. To reduce bias in accounting for the order of cofirst authors, we used recommendations by Casadevall et al, "Reducing bias: accounting for the order of co-first authors." Specifically, in this study, a decision was made based on the most hours worked.

DECLARATION OF COMPETING INTERESTS

There are no competing interests to disclose.

DATA AVAILABILITY

All data are available in the main text, supplementary material, or upon request.

ORCID

Marcel Benkhoff https://orcid.org/0000-0001-6107-7421

REFERENCES

[1] Jones DA, Wright P, Alizadeh MA, Fhadil S, Rathod KS, Guttmann O, Knight C, Timmis A, Baumbach A, Wragg A, Mathur A, Antoniou S. The use of novel oral anticoagulants compared to vitamin K antagonists (warfarin) in patients with left ventricular thrombus after acute myocardial infarction. *Eur Heart J Cardiovasc Pharmacother*. 2021;7:398–404.

[2] Male C, Lensing AWA, Palumbo JS, Kumar R, Nurmeev I, Hege K, Bonnet D, Connor P, Hooimeijer HL, Torres M, Chan AKC, Kenet G, Holzhauer S, Santamaría A, Amedro P, Chalmers E, Simioni P, Bhat RV, Yee DL, Lvova O, et al. Rivaroxaban compared with standard anticoagulants for the treatment of acute venous thromboembolism in children: a randomised, controlled, phase 3 trial. *Lancet Haematol*. 2020;7:e18–27. https://doi.org/10.1016/s2352-3026(19)30219-4

[3] Guimarães HP, Lopes RD, de Barros ESilva PGM, Liporace IL, Sampaio RO, Tarasoutchi F, Hoffmann-Filho CR, de Lemos Soares Patriota R, Leiria TLL, Lamprea D, Precoma DB, Atik FA, Silveira FS, Farias FR, Barreto DO, Almeida AP, Zilli AC, de Souza Neto JD, Cavalcante MA, Figueira FAMS, et al. Rivaroxaban in patients with atrial fibrillation and a bioprosthetic mitral valve. *N Engl J Med*. 2020;383:2117–26.

[4] Carnicelli AP, Hong H, Connolly SJ, Eikelboom J, Giugliano RP, Morrow DA, Patel MR, Wallentin L, Alexander JH, Cecilia Bahit M, Benz AP, Bohula EA, Chao TF, Dyal L, Ezekowitz M, A A, Fox K, Gencer B, Halperin JL, Hijazi Z, Hohnloser SH, et al. Direct oral anticoagulants versus warfarin in patients with atrial fibrillation: patient-level network meta-analyses of randomized clinical trials with interaction testing by age and sex. *Circulation*. 2022;145:242–55.

[5] Lopes RD, Heizer G, Aronson R, Vora AN, Massaro T, Mehran R, Goodman SG, Windecker S, Darius H, Li J, Averkov O, Bahit MC, Berwanger O, Budaj A, Hijazi Z, Parkhomenko A, Sinnaeve P, Storey RF, Thiele H, Vinereanu D, et al. Antithrombotic therapy after acute coronary syndrome or PCI in atrial fibrillation. *N Engl J Med*. 2019;380:1509–24.

[6] Patel MR, Mahaffey KW, Garg J, Pan G, Singer DE, Hacke W, Breithardt G, Halperin JL, Hankey GJ, Piccini JP, Becker RC, Nessel CC, Paolini JF, Berkowitz SD, Fox KA, Califf RM, ROCKET AF Investigators. Rivaroxaban versus warfarin in nonvalvular atrial fibrillation. *N Engl J Med*. 2011;365:883–91.

[7] Giugliano RP, Ruff CT, Braunwald E, Murphy SA, Wiviott SD, Halperin JL, Waldo AL, Ezekowitz MD, Weitz JI, Špinar J, Ruzyllo W, Ruda M, Koretsune Y, Betcher J, Shi M, Grip LT, Patel SP, Patel I, Hanyok JJ, Mercuri M, et al. Edoxaban versus warfarin in patients with atrial fibrillation. *N Engl J Med*. 2013;369:2093–104.

[8] Granger CB, Alexander JH, McMurray JJ, Lopes RD, Hylek EM, Hanna M, Al-Khalidi HR, Ansell J, Atar D, Avezum A, Bahit MC, Diaz R, Easton JD, Ezekowitz JA, Flaker G, Garcia D, Geraldes M, Gersh BJ, Golitsyn S, Goto S, et al. Apixaban versus warfarin in patients with atrial fibrillation. *N Engl J Med*. 2011;365:981–92.

[9] Ten Cate H, Guzik TJ, Eikelboom J, Spronk HMH. Pleiotropic actions of factor Xa inhibition in cardiovascular prevention: mechanistic insights and implications for anti-thrombotic treatment. *Cardiovasc Res*. 2021;117:2030–44.

[10] Achilles A, Mohring A, Dannenberg L, Grandoch M, Hohlfeld T, Fischer JW, Levkau B, Kelm M, Zeus T, Polzin A. Dabigatran enhances platelet reactivity and platelet thrombin receptor expression in patients with atrial fibrillation. *J Thromb Haemost*. 2017;15:473–6.

[11] Polzin A, Dannenberg L, Thienel M, Orban M, Wolff G, Hohlfeld T, Zeus T, Kelm M, Petzold T. Noncanonical effects of oral thrombin and factor Xa inhibitors in platelet activation and arterial thrombosis. *Thromb Haemost*. 2021;121:122–30.

[12] Connolly SJ, Ezekowitz MD, Yusuf S, Eikelboom J, Oldgren J, Parekh A, Pogue J, Reilly PA, Themeles E, Varrone J, Wang S, Alings M, Xavier D, Zhu J, Diaz R, Lewis BS, Darius H, Diener HC, Joyner CD, Wallentin L, et al. Dabigatran versus warfarin in patients with atrial fibrillation. *N Engl J Med*. 2009;361:1139–51.

[13] Petzold T, Thienel M, Dannenberg L, Mourikis P, Helten C, Ayhan A, M'Pembele R, Achilles A, Trojovky K, Konsek D, Zhang Z, Regenauer R, Pircher J, Ehrlich A, Lüsebrink E, Nicolai L, Stocker TJ, Brandl R, Röschenthaler F, Strecker J, et al. Rivaroxaban reduces arterial thrombosis by inhibition of FXa-driven platelet activation via protease activated receptor-1. *Circ Res*. 2020;126:486–500.

[14] Mazzone PM, Capodanno D. Low dose rivaroxaban for the management of atherosclerotic cardiovascular disease. *J Thromb Thrombolysis*. 2023;56:91–102.

[15] Stark K, Massberg S. Interplay between inflammation and thrombosis in cardiovascular pathology. *Nat Rev Cardiol*. 2021;18:666–82.

[16] Gadi I, Fatima S, Elwakiel A, Nazir S, Mohanad Al-Dabet M, Rana R, Bock F, Manoharan J, Gupta D, Biemann R, Nieswandt B, Braun-Dullaeus R, Besler C, Scholz M, Geffers R, Griffin JH, Esmon CT, Kohli S, Isermann B, Shahzad K. Different DOACs control inflammation in cardiac ischemia-reperfusion differently. *Circ Res*. 2021;128:513–29.

[17] Meinel TR, Frey S, Arnold M, Kendroud S, Fischer U, Kaesmacher J, Heldner MR, Jung S. Clinical presentation, diagnostic findings and management of cerebral ischemic events in patients on treatment with non-vitamin K antagonist oral anticoagulants - a systematic review. *PLOS ONE*. 2019;14:e0213379. https://doi.org/10.1371/journal.pone.0213379

[18] Mezger M, Nording H, Sauter R, Graf T, Heim C, von Bubnoff N, Ensminger SM, Langer HF. Platelets and immune responses during thromboinflammation. *Front Immunol*. 2019;10:1731.

[19] Carestia A, Kaufman T, Schattner M. Platelets: new bricks in the building of neutrophil extracellular traps. *Front Immunol*. 2016;7:271.

[20] Wienkamp AK, Erpenbeck L, Rossaint J. Platelets in the NETworks interweaving inflammation and thrombosis. *Front Immunol*. 2022;13:953129.

[21] Kopytek M, Kolasa-Trela R, Ząbczyk M, Undas A, Natorska J. NETosis is associated with the severity of aortic stenosis: Links with inflammation. *Int J Cardiol*. 2019;286:121–6.

[22] Shao Y, Guo Z, Yang Y, Liu L, Huang J, Chen Y, Li L, Sun B. Neutrophil extracellular traps contribute to myofibroblast differentiation and scar hyperplasia through the toll-like receptor 9/nuclear factor Kappa-B/interleukin-6 pathway. *Burns Trauma*. 2022;10:tkac044.

[23] Denorme F, Portier I, Rustad JL, Cody MJ, de Araujo CV, Hoki C, Alexander MD, Grandhi R, Dyer MR, Neal MD, Majersik JJ, Yost CC, Campbell RA. Neutrophil extracellular traps regulate ischemic stroke brain injury. *J Clin Invest*. 2022;132.

[24] Bode MF, Auriemma AC, Grover SP, Hisada Y, Rennie A, Bode WD, Vora R, Subramaniam S, Cooley B, Andrade-Gordon P, Antoniak S, Mackman N. The factor Xa inhibitor rivaroxaban reduces cardiac dysfunction in a mouse model of myocardial infarction. *Thromb Res*. 2018;167:128–34.

[25] Ding Y, Li X, Zhou M, Cai L, Tang H, Xie T, Shi Z, Fu W. Factor Xa inhibitor rivaroxaban suppresses experimental abdominal aortic aneurysm progression via attenuating aortic inflammation. *Vascul Pharmacol*. 2021;136:106818.

[26] Busch G, Seitz I, Steppich B, Hess S, Eckl R, Schömig A, Ott I. Coagulation factor Xa stimulates interleukin-8 release in endothelial cells and mononuclear leukocytes: implications in acute myocardial infarction. *Arterioscler Thromb Vasc Biol*. 2005;25:461–6.

[27] Stolz L, Derouiche A, Devraj K, Weber F, Brunkhorst R, Foerch C. Anticoagulation with warfarin and rivaroxaban ameliorates experimental autoimmune encephalomyelitis. *J Neuroinflammation*. 2017;14:152.

[28] Kondo H, Abe I, Fukui A, Saito S, Miyoshi M, Aoki K, Shinohara T, Teshima Y, Yufu K, Takahashi N. Possible role of rivaroxaban in attenuating pressure-overload-induced atrial fibrosis and fibrillation. *J Cardiol*. 2018;71:310–9.

[29] Schneckmann R, Döring M, Gerfer S, Gorressen S, Heitmeier S, Helten C, Polzin A, Jung C, Kelm M, Fender AC, Flögel U, Grandoch M. Rivaroxaban attenuates neutrophil maturation in the bone marrow niche. *Basic Res Cardiol*. 2023;118:31.

[30] Menter DG, Kopetz S, Hawk E, Sood AK, Loree JM, Gresele P, Honn KV. Platelet "first responders" in wound response, cancer, and metastasis. *Cancer Metastasis Rev*. 2017;36:199–213.

[31] Liu Y, Gao XM, Fang L, Jennings NL, Su Y, Q X, Samson AL, Kiriazis H, Wang XF, Shan L, Sturgeon SA, Medcalf RL, Jackson SP, Dart AM, Du XJ. Novel role of platelets in mediating inflammatory responses and ventricular rupture or remodeling following myocardial infarction. *Arterioscler Thromb Vasc Biol*. 2011;31:834–41.

[32] Ziegler M, Alt K, Paterson BM, Kanellakis P, Bobik A, Donnelly PS, Hagemeyer CE, Peter K. Highly sensitive detection of minimal cardiac ischemia using positron emission tomography imaging of activated platelets. *Sci Rep*. 2016;6:38161.
[33] Yang BC, Mehta JL. Platelet-derived adenosine contributes to the cardioprotective effects of platelets against ischemia-reperfusion injury in isolated rat heart. *J Cardiovasc Pharmacol*. 1994;24:779–85.
[34] Frangogiannis NG, Ren G, Dewald O, Zymek P, Haudek S, Koerting A, Winkelmann K, Michael LH, Lawler J, Entman ML. Critical role of endogenous thrombospondin-1 in preventing expansion of healing myocardial infarcts. *Circulation*. 2005;111:2935–42.
[35] Serhan CN, Sheppard KA. Lipoxin formation during human neutrophil-platelet interactions. Evidence for the transformation of leukotriene A4 by platelet 12-lipoxygenase in vitro. *J Clin Invest*. 1990;85:772–80.
[36] Abdulnour RE, Dalli J, Colby JK, Krishnamoorthy N, Timmons JY, Tan SH, Colas RA, Petasis NA, Serhan CN, Levy BD. Maresin 1 biosynthesis during platelet-neutrophil interactions is organ-protective. *Proc Natl Acad Sci U S A*. 2014;111:16526–31.
[37] Basil MC, Levy BD. Specialized pro-resolving mediators: endogenous regulators of infection and inflammation. *Nat Rev Immunol*. 2016;16:51–67.
[38] Mehta JL, Yang BC, Strates BS, Mehta P. Role of TGF-beta1 in platelet-mediated cardioprotection during ischemia-reperfusion in isolated rat hearts. *Growth Factors*. 1999;16:179–90.
[39] Chen D, Xia Y, Zuo K, Wang Y, Zhang S, Kuang D, Duan Y, Zhao X, Wang G. between SDF-1/CXCR4 and SDF-1/CXCR7 in cardiac stem cell migration. *Sci Rep*. 2015;5:16813.
[40] Sharda A, Flaumenhaft R. The life cycle of platelet granules. *F1000Res*. 2018;7:236.
[41] Novotny J, Oberdieck P, Titova A, Pelisek J, Chandraratne S, Nicol P, Hapfelmeier A, Joner M, Maegdefessel L, Poppert H, Pircher J, Massberg S, Friedrich B, Zimmer C, Schulz C, Boeckh-Behrens T. Thrombus NET content is associated with clinical outcome in stroke and myocardial infarction. *Neurology*. 2020;94(22):e2346–60.
[42] Ellinghaus P, Perzborn E, Hauenschild P, Gerdes C, Heitmeier S, Visser M, Summer H, Laux V. Expression of pro-inflammatory genes in human endothelial cells: comparison of rivaroxaban and dabigatran. *Thromb Res*. 2016;142:44–51.
[43] Martins GL, Duarte RCF, Vieira ÉLM, Rocha NP, Figueiredo EL, Silveira FR, Caiaffa JRS, Lanna RP, Carvalho MDG, Palotás A, Ferreira CN, Reis HJ. Comparison of inflammatory mediators in patients with atrial fibrillation using warfarin or rivaroxaban. *Front Cardiovasc Med*. 2020;7:114.
[44] Gliem M, Hermsen D, van Rooijen N, Hartung HP, Jander S. Secondary intracerebral hemorrhage due to early initiation of oral anticoagulation after ischemic stroke: an experimental study in mice. *Stroke*. 2012;43:3352–7.
[45] Polgár J, Chung SH, Reed GL. Vesicle-associated membrane protein 3 (VAMP-3) and VAMP-8 are present in human platelets and are required for granule secretion. *Blood*. 2002;100:1081–3.
[46] Ren Q, Barber HK, Crawford GL, Karim ZA, Zhao C, Choi W, Wang CC, Hong W, Whiteheart SW. Endobrevin/VAMP-8 is the primary v-SNARE for the platelet release reaction. *Mol Biol Cell*. 2007;18:24–33.
[47] Graham GJ, Ren Q, Dilks JR, Blair P, Whiteheart SW, Flaumenhaft R. Endobrevin/VAMP-8-dependent dense granule release mediates thrombus formation in vivo. *Blood*. 2009;114:1083–90.
[48] Mamas MA, Batson S, Pollock KG, Grundy S, Matthew A, Chapman C, Manuel JA, Farooqui U, Mitchell SA. Meta-analysis comparing apixaban versus rivaroxaban for management of patients with nonvalvular atrial fibrillation. *Am J Cardiol*. 2022;166:58–64.
[49] Russo V, Fabiani D. Put out the fire: The pleiotropic anti-inflammatory action of non-vitamin K oral anticoagulants. *Pharmacol Res*. 2022;182:106335.
[50] Percie du Sert N, Hurst V, Ahluwalia A, Alam S, Avey MT, Baker M, Browne WJ, Clark A, Cuthill IC, Dirnagl U, Emerson M, Garner P, Holgate ST, Howells DW, Karp NA, Lazic SE, Lidster K, MacCallum CJ, Macleod M, Pearl EJ, et al. The ARRIVE guidelines 2.0: updated guidelines for reporting animal research. *Br J Pharmacol*. 2020;177:3617–24.
[51] Terry CM, He Y, Cheung AK. Rivaroxaban improves patency and decreases inflammation in a mouse model of catheter thrombosis. *Thromb Res*. 2016;144:106–12.
[52] Ichikawa H, Shimada M, Narita M, Narita I, Kimura Y, Tanaka M, Osanai T, Okumura K, Tomita H. Rivaroxaban, a direct factor Xa inhibitor, ameliorates hypertensive renal damage through inhibition of the inflammatory response mediated by protease-activated receptor pathway. *J Am Heart Assoc*. 2019;8:e012195. https://doi.org/10.1161/jaha.119.012195
[53] Polzin A, Dannenberg L, Benkhoff M, Barcik M, Keul P, Helten C, Zeus T, Kelm M, Levkau B. S1P lyase inhibition starting after ischemia/reperfusion improves postischemic cardiac remodeling. *JACC Basic Transl Sci*. 2022;7:498–9.
[54] Dannenberg L, Trojovsky K, Ayhan A, Helten C, Zako S, M'Pembele R, Mourikis P, Benkhoff M, Ignatov D, Sarabhai T, Petzold T, Huhn-Wientgen R, Zeus T, Kelm M, Levkau B, Polzin A. MTX treatment does not improve outcome in mice with AMI. *Pharmacology*. 2021;106:225–32.
[55] Zhao X, Ho D, Gao S, Hong C, Vatner DE, Vatner SF. Arterial pressure monitoring in mice. *Curr Protoc Mouse Biol*. 2011;1:105–22.
[56] Heiss C, Sievers RE, Amabile N, Momma TY, Chen Q, Natarajan S, Yeghiazarians Y, Springer ML. In vivo measurement of flow-mediated vasodilation in living rats using high-resolution ultrasound. *Am J Physiol Heart Circ Physiol*. 2008;294:H1086–93.
[57] Chen Q, Sievers RE, Varga M, Kharait S, Haddad DJ, Patton AK, Delany CS, Mutka SC, Blonder JP, Dubé GP, Rosenthal GJ, Springer ML. Pharmacological inhibition of S-nitrosoglutathione reductase improves endothelial vasodilatory function in rats in vivo. *J Appl Physiol (1985)*. 2013;114:752–60.
[58] Vornholz L, Nienhaus F, Gliem M, Alter C, Henning C, Lang A, Ezzahoini H, Wolff G, Clasen L, Rassaf T, Flögel U, Kelm M, Gerdes N, Jander S, Bönner F. Acute heart failure after reperfused ischemic stroke: association with systemic and cardiac inflammatory responses. *Front Physiol*. 2021;12:782760.
[59] Ibanez B, Aletras AH, Arai AE, Arheden H, Bax J, Berry C, Bucciarelli-Ducci C, Croisille P, Dall'Armellina E, Dharmakumar R, Eitel I, Fernández-Jiménez R, Friedrich MG, García-Dorado D, Hausenloy DJ, Kim RJ, Kozerke S, Kramer CM, Salerno M, Sánchez-González J, et al. Cardiac MRI endpoints in myocardial infarction experimental and clinical trials: JACC Scientific Expert Panel. *J Am Coll Cardiol*. 2019;74:238–56.
[60] Stone GW, Selker HP, Thiele H, Patel MR, Udelson JE, Ohman EM, Maehara A, Eitel I, Granger CB, Jenkins PL, Nichols M, Ben-Yehuda O. Relationship between infarct size and outcomes following primary PCI: patient-level analysis from 10 randomized trials. *j Am Coll Cardiol*. 2016;67:1674–83.
[61] Leuschner G, Mayr CH, Ansari M, Seeliger B, Frankenberger M, Kneidinger N, Hatz RA, Hilgendorff A, Prasse A, Behr A, Mann M, Schiller HB. A proteomics workflow reveals predictive autoantigens in idiopathic pulmonary fibrosis. *medRxiv*. 2021;2021, 02.17.21251826.
[62] Cox J, Hein MY, Luber CA, Paron I, Nagaraj N, Mann M. Accurate proteome-wide label-free quantification by delayed normalization and maximal peptide ratio extraction, termed MaxLFQ. *Mol Cell Proteomics*. 2014;13:2513–26.
[63] Ritchie ME, Phipson B, Wu D, Hu Y, Law CW, Shi W, Smyth GK. limma powers differential expression analyses for RNA-sequencing and microarray studies. *Nucleic Acids Res*. 2015;43:e47. https://doi.org/10.1093/nar/gkv007

[64] Stekhoven DJ, Bühlmann P. MissForest–non-parametric missing value imputation for mixed-type data. *Bioinformatics*. 2012;28:112–8.
[65] Bates D, Mächler M, Bolker B, Walker S. Fitting Linear mixed-effects models using lme4. *J Stat Soft*. 2014;arXiv:1406.
[66] Kuznetsova A, Brockhoff P, Christensen R. LmerTest: tests in linear mixed effects models. *R Package Version*. 2015;2.
[67] Xie Z, Bailey A, Kuleshov MV, Clarke DJB, Evangelista JE, Jenkins SL, Lachmann A, Wojciechowicz ML, Kropiwnicki E, Jagodnik KM, Jeon M, Ma'ayan A. Gene set knowledge discovery with Enrichr. *Curr Protoc*. 2021;1:e90. https://doi.org/10.1002/cpz1.90

SUPPLEMENTARY MATERIAL

The online version contains supplementary material available at https://doi.org/10.1016/j.jtha.2024.10.025